J. Fluid Mech. (2009), *vol.* 625, *pp.* 371–385.
doi:10.1017/S002211200900620X Printed in the United Kingdom

Clusters of sedimenting high-Reynolds-number particles

W. BRENT DANIEL[1], ROBERT E. ECKE[1], G. SUBRAMANIAN[2]† AND DONALD L. KOCH[3]

[1]Center for Nonlinear Studies and Condensed Matter and Thermal Physics, Los Alamos National Laboratory, P.O. Box 1663, Los Alamos, NM 87545, USA

[2]Engineering Mechanics Unit, Jawaharlal Nehru Centre for Advanced Scientific Research, Jakkur, Bangalore 560064, India

[3]School of Chemical and Biomolecular Engineering, Cornell University, Ithaca, NY 14853, USA

(Received 13 February 2008 and in revised form 16 December 2008)

We report experiments wherein groups of particles were allowed to sediment in an otherwise quiescent fluid contained in a large tank. The Reynolds number of the particles, defined as $Re = aU/\nu$, ranged from 93 to 425; here, a is the radius of the spherical particle, U its settling velocity and ν the kinematic viscosity of the fluid. The characteristic size of a cluster, in a plane transverse to gravity, was measured by a 'cluster variance' ($\langle r_t^2 \rangle$); the latter is defined as the mean square of the transverse coordinates of all constituent particles, averaged over a series of runs. The cluster variance, when plotted as a function of time, exhibited two regimes. There was a quadratic growth in the variance at short times ($\langle r_t^2 \rangle \propto t^2$), while for long times, the cluster variance exhibited a slower sublinear growth with $\langle r_t^2 \rangle \propto t^{0.67}$. A theory, based on isotropic repulsive hydrodynamic interactions between particles, predicts the cluster variance to grow as $t^{2/3}$ in the limit of long times. The theoretical framework was originally proposed to describe the long-time self-similar evolution of dilute clusters in the limit $Re \ll 1$ Subramanian & Koch (*J. Fluid Mech.*, vol. 603, 2008, p. 63), when the probability of wake-mediated interactions between particles remains asymptotically small; the latter requirement is satisfied for homogeneous spherical clusters larger than a critical radius, and is evidently satisfied for planar clusters oriented transversely to gravity. The isotropy of the interactions therefore stems from the isotropy, at large distances, of the disturbance velocity field produced by a single sedimenting particle outside its wake (which contains the compensating inflow to satisfy mass conservation). Herein, the theory is extended to large Re using an empirical correlation for the drag on a sedimenting particle. This allows one to predict, as a function of Re, the numerical prefactors in the expressions for the cluster variance of both spherical and planar clusters; the predictions for the growth exponent remain unchanged. The agreement between the theoretical and experimental growth exponents supports the hypothesis of a self-similar expansion at long times. The prefactor determined from the experimental observations is found to lie between the theoretical predictions for planar and spherical clusters.

1. Introduction

In an earlier paper (Subramanian & Koch 2008), the evolution of dilute clusters of sedimenting particles, on account of interparticle hydrodynamic interactions, was

† Email address for correspondence: sganesh@jncasr.ac.in

analysed theoretically in the limit when Re is small but finite. Here, $Re = aU/\nu$ is the particle Reynolds number, where a is the particle size (radius), U is its settling velocity and ν is the kinematic viscosity of the ambient fluid. The cluster evolves as each constituent particle, in a reference frame moving with its terminal velocity, is convected by the disturbance velocity fields produced by all other particles. In the absence of wake-mediated interactions, both spherical and planar clusters, the latter with their plane oriented transversely to gravity, were found to eventually expand in a self-similar manner with the cluster variance increasing as $\langle r^2 \rangle \propto t^{2/3}$, t being the time. This expansion results from source-flow interactions prevalent outside the particle wakes. The cluster variance $\langle r^2 \rangle$ is a mean-square measure of the cluster size; thus $\langle r^2 \rangle = 4\pi/N \int_0^{R_{cl}} [r^2 n(r,t)] r^2 \mathrm{d}r$ for a spherical cluster, and $\langle r^2 \rangle = 2\pi/N \int_0^{R_{cl}} [r^2 n(r,t)] r \mathrm{d}r$ for a planar cluster, where N is the total number of particles, and $n(r,t)$ is the number density field (volumetric or areal) in the cluster of radius R_{cl}. However, with the intent of comparing the above theoretical predictions to the experimental measurements discussed here, we focus on the mean-square extent of the cluster in a plane transverse to gravity ($\langle r_t^2 \rangle$); we shall, for the most part, continue to call this the cluster variance except in cases where we need to differentiate it from $\langle r^2 \rangle$. For a planar cluster oriented transversely to gravity, the mean-square extent is, of course, that in a transverse plane. For a spherical cluster, on the other hand, the mean-square extent in a transverse plane may be defined as $\langle r_t^2 \rangle = 2\pi/N \int_0^{R_{cl}} r^2 \, \mathrm{d}r \int_0^{\pi} \sin\theta \mathrm{d}\theta (r^2 \sin^2\theta) n(r,t)$, where $r \sin\theta$ is the projection, onto a transverse plane, of the actual radial distance, θ being the polar angle defined with respect to the vertical. For a spherically symmetric number density field, as is the case in theory, $\langle r_t^2 \rangle$ is related to $\langle r^2 \rangle$ as $\langle r_t^2 \rangle = 2/3 \langle r^2 \rangle$; this may easily be seen by evaluating the aforementioned integral over the polar angle. The predictions of the modified theoretical analysis for $\langle r_t^2 \rangle$ at large Re are supported by experimental observations reported in this paper.

In the experiments, small groups of particles were allowed to sediment under gravity in an otherwise quiescent fluid, and the size of the sedimenting clusters was monitored as a function of time. The clusters were observed to grow in their transverse dimensions. For long times, the variance, as measured in a transverse plane, was found to grow as $t^{0.67}$, in close agreement with the aforementioned theory. In the experiments, the cluster variance is calculated as the mean square of the transverse coordinates of all cluster particles averaged over several runs. The reason for the agreement between the experimental and theoretical long-time growth exponents is not readily evident, since the original theory is rigorously valid only in the limit $Re \ll 1$, while the Reynolds numbers of the particles used in the experiments were quite large (93–425). However, an empirical modification of the original low-Re theory allows one to bridge this gap in Re. The empirical input needed is the expression for the drag on a sedimenting particle as a function of Re, obtainable from standard sources (for instance, see Clift, Grace & Weber 1978); this then characterizes the dependence on Re of the strength of the interparticle interactions. The empirical input does not alter the long-time growth exponent, but allows one to predict, as a function of Re, the numerical prefactor multiplying $t^{2/3}$ in the expression for the cluster variance. The resulting predictions for planar and spherical clusters are found to bracket the experimental results. Agreement between the theory and experiment suggests that the underlying physical mechanism for the slow expansion of sufficiently dilute clusters of sedimenting particles may remain the same regardless of Re.

The paper is organized as follows. In the next section, we first discuss details of the experimental setup and measurement procedure. The variance of a cluster comprising 60 particles with $Re = 93$, as calculated from data averaged over a series of runs, is then plotted as a function of time. The plot exhibits a short-time regime when the variance grows quadratically, followed by a long-time regime of slower sublinear growth. Plots for the variances of other clusters used in the experiments, with differing number of particles (10–80), reveal a similar dynamical behaviour, although the crossover time from the quadratic to the sublinear regime does depend on the number of particles in the cluster. In § 3, a theoretical framework, based on isotropic repulsive hydrodynamic interactions at finite Re between particles in a dilute cluster, is proposed to explain the sublinear growth observed in the experiments. As mentioned earlier, the theory is a simple empirical extension of the analysis in Subramanian & Koch (2008); the latter examined the long-time expansion of axisymmetric planar clusters and spherical clusters at small Re. We therefore summarize the main results of the low-Re analysis to begin with, and then mention the modifications necessary to characterize the expansion of sedimenting clusters at higher Re. The predictions of the modified theory for the variance of spherical and planar clusters is shown to bracket the experimental observations. In § 4, we end with some conclusions.

2. Experiments

The nature of interparticle hydrodynamic interactions at finite Re was studied experimentally via clusters of millimetre-sized spherical particles dropped through a quiescent tank of water at room temperature. The tank was 61 cm deep with an hexagonal cross-section measuring 46 cm between parallel sides. A diagram of the apparatus is shown in figure 1. Particles were loaded into a cylindrical reservoir machined in clear polycarbonate sheet. An aperture was cut in a second sheet mounted beneath the first. The aperture was slid into place beneath the reservoir to release the particles at the beginning of each drop. Particles used in the experiments had diameters of 1 mm, 1.588 mm and 2.381 mm, corresponding to Reynolds numbers of 93, 216 and 425, respectively, based on terminal velocities of 8.6, 27.3 and 35.7 cm s^{-1}; the density (1.0 g cm^{-3}) and viscosity (0.01 cm^2 s^{-1}) of water at room temperature were used in obtaining the values of the Reynolds number. The particles were made of silicon nitride with a standard deviation in their diameters of less than 1.3 μm (not more than 0.05 % to 0.1 % of the diameter); the density of the particles was 3.23 g $cm^{-}3$ (ρ_p) with a standard deviation of 0.7 %. These variations in particle size and density lead to a distribution of terminal velocities of less than 1 %. The maximum cluster diameter was 6.5 cm, less than 2 % of the cell cross-sectional area. The areal fraction of the sum of the particle cross-sections was even smaller, less than 0.2 %. The resulting back-flow velocity was less than 0.2 cm s^{-1}, much smaller than the terminal settling velocities of the individual particles. (As discussed in the next section, for long times, the settling velocity of the cluster is of the same order of magnitude as that of a single particle.) Thus, back-flow effects are expected to play a minor role in the particle evolution described below.

The evolution of the sedimenting cluster was observed via an angled mirror placed directly below the cluster's path of travel. Particle images, projected onto the plane transverse to gravity, were captured at 60 frames per second on a 1.3 mega-pixel video camera. In figure 2, images of sedimenting clusters are shown at three different times from the side (left) and bottom (right) during runs with $Re = 93$ and $N = 19$ and 20, respectively. The particle images were thresholded and the mean-square variance

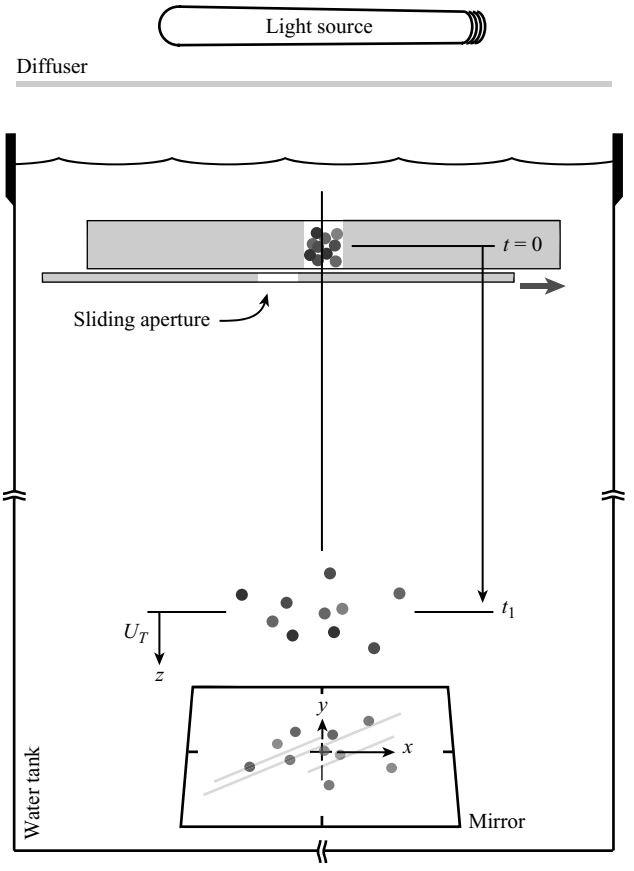

FIGURE 1. A schematic illustration of the experiment. Particle silhouettes were imaged in a mirror directly below the tank.

of the darkened pixels was computed. This approach avoided experimental difficulties in uniquely identifying each particle, but did introduce potential errors as a result of under-counting pixels when particle images overlapped. The induced error was largest at early times.

The error in the cluster variance associated with overlapping images may be estimated as follows. The correct cluster variance, in terms of the variance of the darkened pixel field, may be written as

$$\langle r^2 \rangle = (2\pi/N_{pix}) \int_0^{R_{cl}} n_{pix} r_t^3 \, \mathrm{d}r_t, \tag{2.1}$$

where n_{pix} is the areal density, and N_{pix} is the number of pixels, both corresponding to the total number of particles (N) as opposed to the number of visible ones (N_v), and r_t as before denotes the radial distance in a transverse plane; assuming the number of particles per unit volume of the cluster to be independent of r, the areal density of the particles is given by $n_a = 3N/2\pi R_{cl}^3 (R_{cl}^2 - r_t^2)^{1/2}$. Denoting the area of a single pixel as a_{pix}, we then have $N_{pix} a_{pix} = N(\pi a^2)$ and $n_{pix} a_{pix} = 3Na^2/2R_{cl}^3 (R_{cl}^2 - r_t^2)^{1/2}$. Now, n_{pix} may be expressed as a sum of the visible pixel areal density (n_{pix}^v) and the overlap pixel areal density (n_{pix}^o), an overlap pixel being defined as a pixel where the

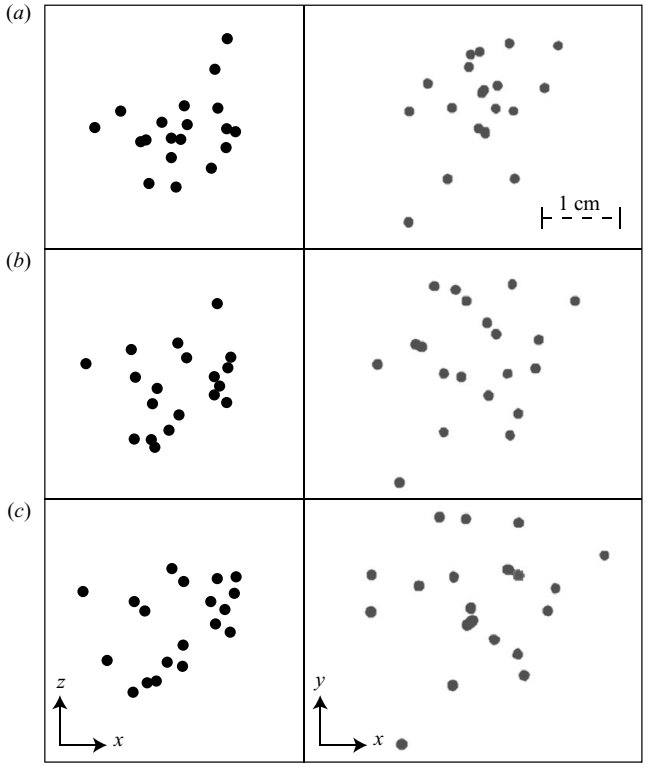

FIGURE 2. Particle images projected onto a plane parallel to gravity (left) and projected onto a plane transverse to gravity (right) for typical experimental runs with $Re = 93$ and $N = 19$ (left) and $N = 20$ (right). The evolution times are (*a*) 1.0 s, (*b*) 1.5 s, and (*c*) 2 s. The images are perspective corrected and filtered for better individual particle identification.

images of two or more particles (projected onto the transverse plane) overlap. Thus, $\langle r^2 \rangle = (2\pi/N_{pix}) \int_0^{R_{cl}} (n^v_{pix} + n^o_{pix}) r_t^3 \mathrm{d}r_t$, where the contributions corresponding to the overlap and visible pixels may now be calculated. Since the probability of occurrence of an overlap pixel, approximated as the probability of occurrence of pair overlaps (of images), is given by $9N^2a^4/4R_{cl}^6(R_{cl}^2 - r_t^2)$, one may write

$$\langle r^2 \rangle_{overlap} = \frac{(2\pi)}{N_{pix}} \int_0^{R_{cl}} n^o_{pix} r_t^3 \mathrm{d}r_t, \tag{2.2}$$

$$= \frac{2}{Na^2} \int_0^{R_{cl}} \frac{9N^2a^4}{4R_{cl}^6} \left(R_{cl}^2 - r_t^2\right) r_t^3 \mathrm{d}r_t, \tag{2.3}$$

$$= \frac{3Na^2}{8}. \tag{2.4}$$

The calculated cluster variance from the visible pixels is given by

$$\langle r^2 \rangle_{visible} = \frac{(2\pi)}{N_{pix}} \int_0^{R_{cl}} n^v_{pix} r_t^3 \mathrm{d}r_t, \tag{2.5}$$

$$= \frac{2\pi}{Na^2} \int_0^{R_{cl}} \frac{3N_v a^2}{2R_{cl}^3} \left(R_{cl}^2 - r_t^2\right)^{\frac{1}{2}} r_t^3 \mathrm{d}r_t, \tag{2.6}$$

$$= \frac{2}{5} \frac{N_v}{N} R_{cl}^2, \tag{2.7}$$

where $n^v_{pix}a_{pix}$ is given by an expression identical to $n_{pix}a_{pix}$ but with N replaced by N_v. Thus, the relative error in the calculated cluster variance on account of overlapping particle images is given by the ratio of (2.4) to (2.7), being equal to $\frac{15N}{16N_v}\frac{Na^2}{R^2_{cl}}$. This expected error was typically observed to be between 0 and 8 %. Highs of 14 % to 17 % were seen at the earliest time ($t = 0.35$ s) for the $N = 70$ and $N = 80$ drops.

The variance calculation also included a correction for perspective error. Without correction, particles appear larger at the bottom of a run than they do at the top. To compensate, the linear dimension of a camera pixel was measured at the top π_t and at the bottom π_b of the measurement volume by directly imaging a rule positioned at each location. Thresholded pixel coordinates, (r'_x, r'_y), were converted to real-world coordinates via the linear transformation $(r_x, r_y) = \beta(i)\,(r'_x, r'_y)$, where

$$\beta(i) = \pi_t - (\pi_t - \pi_b)\frac{i-1}{N_f - 1}. \tag{2.8}$$

Here, N_f is the total number of image frames captured within the measurement volume and i is the image frame being converted. The correction assumes a uniform cluster settling velocity based on empirical observation.

Ideally, the amount of perspective correction applied to the image of a particle should vary as a function of each individual particle's vertical position in a cluster at a given instant of time (information that was unavailable in this experiment). Instead, all particle positions were mapped at each time step using the linear transformation described above (based on the predicted cluster centre of mass). As a result, a residual error of up to ± 5 %, in the apparent transverse radial position of particles, was incurred at the vertical extremes of the largest clusters via the perspective-correcting mapping. Particles near the top of a cluster contributed less than they should to the measured variance; particles near the bottom contributed more. Assuming that the particle density within a cluster is nearly isotropic, however, a particle whose apparent position has been overcompensated is likely to be balanced by a particle whose apparent position has been equally undercompensated. Thus, the residual impact on the cluster variance is only about ± 0.5 %, even for the largest clusters.

An important consideration with regard to the motion of particles released from rest in a fluid is the time it takes for a single particle to achieve its terminal velocity. The time scale of particle acceleration may be estimated from the equation of motion of a single particle. The latter may be written in the form,

$$\left(\frac{4}{3}\pi\rho_p a^3\right)\frac{\mathrm{d}U}{\mathrm{d}t} + c_s 6\pi\mu a U = (1-\beta)\left(\frac{4}{3}\pi\rho a^3\right) g, \tag{2.9}$$

where $\beta = \rho/\rho_p$ and c_s is an Re-dependent correction to the Stokes drag. Taking the Schiller and Naumann relation from Clift *et al.* (1978) yields $c_s = 1 + 0.242Re^{0.687}$ for $Re < 400$. The steady-state form of this equation predicts the experimentally measured terminal velocities quite well (for $Re = 425$, the correlation overpredicts the experimental value by about 10 %). Solving this equation numerically for the time dependence of particle motion yields the acceleration time scale for the individual particles, i.e. the time to reach terminal velocity. Although the form of the solutions is not strictly exponential, (2.9) being nonlinear, an exponential function with a characteristic time τ nevertheless fits the solutions rather well. One thereby obtains $\tau = 0.021, 0.031$ and 0.045 s corresponding to $Re = 93, 216$ and 425, respectively.

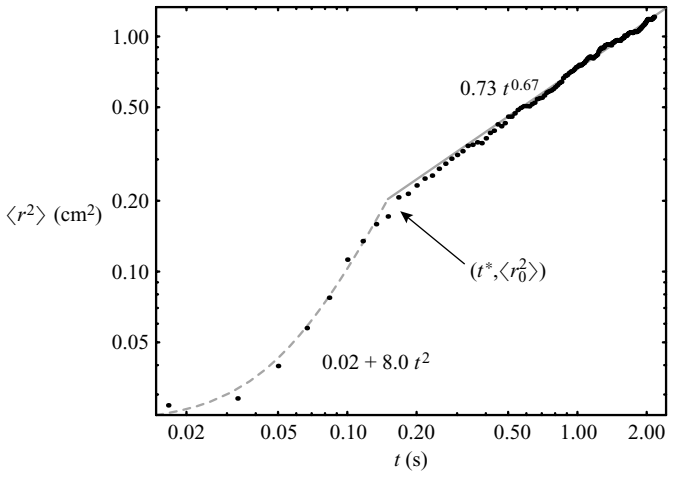

FIGURE 3. Temporal evolution of the cluster variance for a group of 60 particles with $Re = 93$. Two distinct behaviours are seen: a rapid quadratic expansion at small times, followed by a much slower expansion at long times. Here t^* denotes the time of transition between the two regimes.

The temporal evolution of the cluster variance in the transverse plane, calculated in the aforementioned manner, is shown in figure 3 for a single drop of a cluster comprising 60 particles with $Re = 93$. Ten such drops were typically performed for each combination of Re and N. The observed expansion of the clusters falls into two distinct phases: an initial rapid expansion at short times (ranging from 0.1 s to 0.4 s; 0.2 s for the case shown in figure 3), when the variance grows quadratically, followed by a much slower sublinear growth at longer times. The size attained by the cluster at the end of this initial expansion phase depends on N, and the data suggest an inverse correlation. Since the duration of the quadratic expansion regime exceeds 0.1 s for all cases examined, it is readily seen from the above estimates of the particle acceleration time scales that individual particles attain their respective terminal velocities well before the onset of the sublinear growth regime. Thus, one may safely ignore effects associated with the initial particle accelerations when comparing the experimental and theoretical predictions for the cluster variance in the sublinear regime.

The presence of the quadratic growth regime may be related to the dominance of wake interactions in the initial cluster. Wake-mediated interactions of particles at high Re have been referred to as 'draft, kiss and tumble' (DKT) interactions in literature (see Feng, Hu & Joseph 1994; Fortes, Joseph & Lundgren 1987). The name comes about since the trailing particle drafts in the wake of the leading one to begin with, rapidly approaching it from behind, and the particle pair eventually tumbles with subsequent increase in the transverse separation. We again refer to figure 2 for the series of snapshots of clusters of 19 and 20 particles at three different time instants during a run. The dynamics in a typical sedimenting cluster consists of events on two different time scales. The aforementioned DKT pair interactions lead to a rapid local rearrangement in particle positions; this rearrangement is evident from the changes in the positions of interior particles from one snapshot to the other in the (longitudinal) projections parallel to gravity. There is, in addition, a much more gradual increase in the overall cluster dimensions on a longer time scale that leads to the eventual sublinear growth of the cluster variance. Evidence of such an expansion although

present is more subtle in the longitudinal projections. However, the gradual increase in the radial dimensions is much more easily seen in the transverse projections in figure 2.

The theoretical results discussed in the next section attribute this slow expansion to the presence of weak, but long-ranged, isotropic repulsive interactions between sedimenting particles at any finite Re. The resulting prediction for the cluster variance is then compared with the experimental findings. Further, figure 2 also shows that although the aspect ratio of a typical cluster is somewhat less than unity, it is far from being planar. The vertical extent of the observed clusters is, of course, much greater than the vertical spread expected due to the polydispersity in particle sizes and densities. Since the long-ranged isotropic interactions, that drive the eventual sublinear growth, do not act to change the aspect ratio of a cluster, the latter appears to be set by the dynamics of DKT pair interactions. The initial decrease in the vertical separation between two interacting particles during approach acts, on average, to decrease the cluster aspect ratio; on the other hand, the resulting particle pair settles faster than surrounding single particles, and this acts to increase the vertical extent of the cluster. The observed aspect ratio of the clusters in the experiments appears to result from a dynamic balance of these two effects. Comparison with theory in § 3 confirms the non-planarity of the experimental clusters, since the variances determined from experiments are found to lie between the theoretical predictions for spherical and planar clusters.

It was also indirectly verified that the cluster settling velocities were of the same order of magnitude as that of the individual particles. Since the image frames in each data set span the time interval between the instant at which the particles were released until the time at which the first particle made contact with the mirror, the number of image frames contained in each data set gave a reasonable approximation for the cluster fall time. (A rather small error arises because the measurement stops when the lowermost particle, and not the cluster centre of mass, makes contact with the mirror. This has the effect of slightly overestimating the sedimentation velocities of the largest clusters.) The cluster fall time determined in this fashion was found to exhibit no significant dependence on N. This is consistent with the theoretical framework of § 3 which attributes the cluster expansion to far-field isotropic repulsive interactions. The isotropy of the interactions implies that the cluster centre of mass continues to settle at the same rate as a single particle. The insensitivity of the cluster settling velocity to N also eliminates the possibility of additional dynamics on the length (and time) scales of the cluster. Such dynamics is, in fact, well known for clusters in the 'suspension-drop' regime (see Nitsche & Batchelor 1997; Subramanian & Koch 2008), when there is an interior recirculation set up on the length scale of the cluster reminiscent of a translating drop. The suspension-drop regime is, of course, only relevant in the limit $Re \ll 1$. However, similar cluster-scale dynamics might result at higher Re when the motion of a typical typical cluster particle is influenced by the wakes of many other particles. The probability of this occurrence is given by the ratio of the volumes of particle wakes to that of the cluster. For the experimental parameters, this ratio is negligible, so that, as mentioned earlier, the only wake-mediated interactions are of a local nature.

Finally, an additional source of experimental error deserves mention. The act of sliding the aperture into place to initiate a drop necessarily induces flow in the boundary layer just beneath it. For the most part, no noticeable effect was observed either on the trajectories of the particles or on the trajectory of the cluster mean. On rare occasions, single particles would maintain a inclined trajectory at a nearly

constant inclination over the entire duration of the fall. The direction of lateral motion was always consistent with spin-induced lift, as would be caused by the plate inducing a spin on a particle resting against it as the aperture was slid into position. This happened particularly when the aperture plate was opened too slowly, suggesting that the initial lateral motion of a particle due to a spin-induced lift was perhaps maintained by a large-scale coherent motion set up in the tank by the slowly moving plate. Such runs were easily identified in the initial review of the video clip, and the corresponding experimental data discarded.

3. Theory

A theoretical framework was developed in Subramanian & Koch (2008) to describe the evolution of a dilute cluster of sedimenting particles in the limit when Re is small but finite, and when the average separation between particles is much greater than an inertial screening length. The latter denotes the length scale at which convection becomes comparable to viscous diffusion, and scales as aRe^{-1} in the limit $Re \ll 1$; for higher Re, the inertial screening length is $O(a)$. The evolution of the cluster is driven by interparticle interactions which arise on account of disturbance velocity fields generated by the sedimenting particles. At distances from a particle greater than an inertial screening length, this disturbance velocity field has a source-sink character (see Batchelor 1967); the momentum defect brought in via a narrow wake behind the particle is convected radially outwards in the remaining directions. Thus, the character of the far-field velocity disturbance, in a region outside the wake, is that of a source-flow given by

$$u_r = \frac{Q}{4\pi r^2}, \tag{3.1}$$

while the compensating inflow within the narrow wake region behind the spherical particle, given by $(x^2 + y^2) \leqslant O(\nu z/U)$, decays at a slower rate, being

$$u_r \sim -\frac{QU}{6\pi\nu r}, \tag{3.2}$$

close to the wake centreline; here, $Q = 6\pi\nu a$ is source strength in the limit $Re \ll 1$, and z is a vertical coordinate measured against gravity.

Subramanian & Koch (2008) argued that, in the limit of small Re, initially spherical clusters would eventually expand in a self-similar manner, with interactions between cluster particles being dominated by the source part ($O(1/r^2)$) of the disturbance velocity fields. In other words, for long times, each particle, in a reference frame moving with the sedimenting cluster, is passively convected by the weak source fields due to all other cluster particles. Thus, interparticle interactions in the cluster are repulsive, and follow an inverse-square law (see (3.1)). However, wake interactions, dominant during an initial transient, were argued to play a crucial role, even at small Re, in reducing the dimensionality of the ensuing source-field driven expansion. While initially spherical clusters with radii larger than $O(N\nu/U)$ would undergo an isotropic expansion on account of source-field interactions, those with radii much smaller than $O(N\nu/U)$ were predicted to first collapse into a pan-cake configuration on account of wake interactions; the latter configuration then begins to expand, again due to source-field interactions, but now largely restricted to a plane transverse to gravity. N here is again the total number of particles. Analytical expressions for the cluster variance ($\langle r^2 \rangle$) were obtained in the limit of long times for the cases of a spherical

cluster, and an axisymmetric planar cluster; one finds

$$\langle r^2 \rangle = A(NQt)^{2/3}, \tag{3.3}$$

where $A = 0.317$ and 0.231 for planar and spherical clusters, respectively. In the limit $Re \ll 1$, it is reasonable to expect the aforementioned values of A to serve as physical bounds for the long-time rate of expansion of an initially spherical cluster of an arbitrary size. The corresponding variance in a transverse plane ($\langle r_t^2 \rangle$), the quantity of interest in this paper, is given by

$$\langle r_t^2 \rangle = A'(NQt)^{2/3}, \tag{3.4}$$

where $A' = 0.317$ and 0.154 for planar and spherical clusters, respectively.

To extend the above theoretical framework to higher Re relevant to the experiments, we observe that the predicted self-similar expansion hinges on the nature of the velocity field around a single sedimenting particle, and at large distances from it; in particular, its source-like character, leading to repulsive interparticle interactions. This far-field behaviour, however, remains unaltered even at higher Re. The $O(1/r^2)$ source flow at large distances from a sedimenting sphere arises as a compensating effect for inflow via the wake in its rear. The latter is related to the momentum defect associated with the drag exerted on the particle at any Re. Indeed, for any non-lifting translating particle, an integral momentum balance yields the generic relation (see Batchelor 1967):

$$F_D = \rho U Q, \tag{3.5}$$

where ρ is the fluid density, F_D is the magnitude of the drag and Q is the strength of the wake inflow. The resulting source flow is again given by (3.1), where Q, the source-strength, is now a function of Re; thus, Q characterizes the strength of the repulsive source-field interactions in a cluster at finite Re, when the effects of wake interactions are negligible. Of course, on using the Stokes drag in (3.5), one obtains the source strength in the limit $Re \ll 1$, viz. $Q = 6\pi\nu a$. For higher Re, Q may be obtained from any standard correlation for the drag on a translating sphere. Again using the Schiller and Naumann relation from Clift *et al.* (1978), one obtains $Q = 6\pi\nu a(1 + 0.242Re^{0.687})$ for $Re < 400$.

As indicated in the earlier section, constituent particles accelerate to their terminal velocity well before the onset of the self-similar expansion of the cluster. Further, the time scale associated with the relatively weak source-field interactions, that drive the cluster expansion, is much longer than the time scale of particle acceleration. Specifically, a comparison of the time scale of the interaction flow field, $(Q/4\pi R^3)^{-1}$, with the acceleration time scale of a particle, $\tau_p = m/(6\pi\mu a c_s)$ yields the condition, $\rho_p/\rho \ll 3(R/a)^3$, for particle inertia to play a negligible role in the long-time evolution of the cluster; here, R is a typical interparticle separation in the cluster. The above condition is indeed satisfied for the experiments. The cluster variance at finite Re is therefore again given by (3.4) with Q being the source strength at finite Re; one obtains

$$\langle r_t^2 \rangle = 7.08A'[N\nu a(1 + 0.242Re^{0.687})t]^{2/3}. \tag{3.6}$$

The above comparison of time scales implicitly assumes source-field interactions to act in isolation even at higher Re. Although this is not true for arbitrary interparticle separations, the $O(1/r^2)$ source fields are still expected to be dominant at sufficiently large separations; it is, in fact, known that there cannot be a larger contribution to the departure from a uniform stream (Batchelor 1967). Therefore, even at higher Re, the diluteness of the cluster appears to be a sufficient condition for the validity of

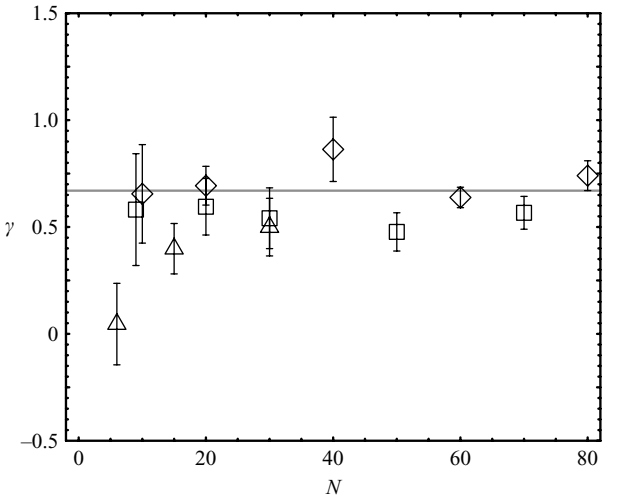

FIGURE 4. The variance in the positions of a group of particles is predicted to increase as $\langle r_i^2 \rangle \propto t^{\gamma}$ with $\gamma = 2/3$ (the solid gray line). The experimentally obtained growth exponents are shown for $Re = 93$ (◇), 216 (□) and 425 (△). The errors bars indicate the r.m.s. variation.

(3.3). A further complication arises at large Reynolds numbers, however, since flows past both fixed and sedimenting particles exhibit qualitative changes in structure at higher Re (see Magarvey & Bishop, 1961; Wu & Faeth, 1993; Natarajan & Acrivos 1993; Ormieres & Provansal 1999). In particular, the flow around a sedimenting sphere is known to undergo a bifurcation at $Re \approx 100$, entailing a loss of axisymmetry of the wake. The resulting plane-symmetric wake undergoes a second bifurcation at $Re \approx 140$ leading to the onset of vortex shedding (see Mittal 1999; Jenny, Dusek & Bouchet 2004; Ghidersa & Dusek 2000); on average, the unsteady wake continues to remain plane symmetric. This departure from axisymmetry should, in principle, lead to a lift force in the plane of symmetry, and therefore a transverse velocity at right angles to the direction of gravity. A non-zero lift force on a single particle and the resulting transverse velocity would, even in the absence of interactions, lead to a quadratic growth of the cluster variance. Provided $Re < 100$, however, one expects (3.4) with the two values of A, and a Q that is now a function of Re, to provide Re-dependent upper and lower bounds for the rate of expansion of a dilute sedimenting cluster, in a transverse plane, in the limit of long times.

Having given a suitably detailed account of the original low-Re theory, and its extension to higher Re, we compare the experimental data for the growth exponent with the theoretical prediction. To begin with, the temporal evolution of the cluster variance, determined from experiments, was fit using the function $A_i' t^{\gamma_i}$ for each drop i and for times beyond the transition time t^*. The mean values of the scaling exponent $\overline{\gamma}$ are plotted in figure 4 for each combination of Re and N. In almost all cases, the experimental exponents are quite close to the theoretical prediction of $\gamma = 2/3$. The farthest outlier is the scaling exponent for $Re = 425$ and $N = 6$. The latter is the smallest value of N used in the experiments. That the exponent in this case lies well below the theoretical prediction must come as no surprise, since the theory is based on a continuum representation of a sedimenting cluster in terms of a number density field; the continuum approximation is expected to break down for small N.

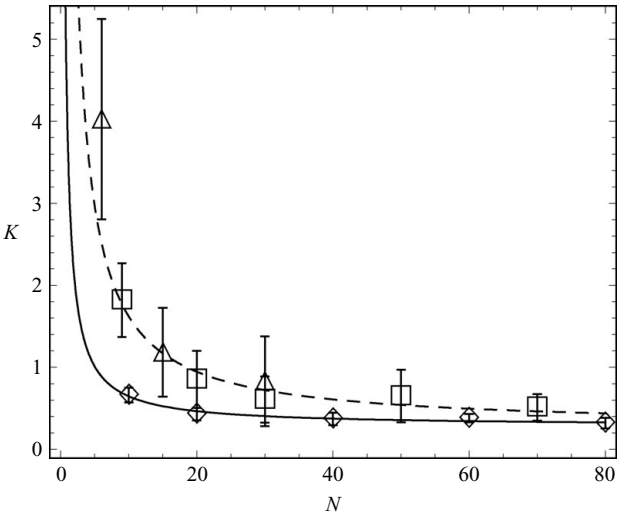

FIGURE 5. Experimentally obtained values of K for $Re = 93$ (◇), 216 (□) and 425 (△). The K values do show a dependence on N and, to a lesser extent, on Re. The curves are fits of the form $K = c(Re)N^{-1} + K_0$ to the $Re = 93$ (solid) and $Re = 216$ (dashed) data.

We now compare the theoretical predictions for the numerical prefactor in (3.6). To this end, we first exploit the fact that, for long times, a sedimenting cluster expands in a quasi-steady self-similar manner, and the drag force on each particle therefore precisely balances the net gravitational force; that is, $F_D = \pi d^3(\rho_p - \rho)g/6$, where $d = 2a$ is the particle diameter. Now, (3.3) may be written as in terms of Q; using $Q = F_D/(\rho U)$ with the above expression for F_D, one obtains the following alternate expression for the cluster variance:

$$\langle r_t^2 \rangle = K \left[\frac{d^4(\rho_p - \rho)g}{6\rho\nu Re} \right]^{2/3} N^{2/3} t^{2/3}, \tag{3.7}$$

where K equals 0.42 and 0.2 for planar and spherical clusters, respectively.

To test the correspondence between the theory and the experimental data, the experimental prefactors were computed from the plots of $\langle r_t^2 \rangle$ versus t using the functional form for the long-time expansion predicted by theory viz. (3.7). That is, one calculates for each data set the quantity

$$K(N, Re) = \langle r_t^2 \rangle \left[\frac{d^4(\rho_p - \rho)g}{6\rho\nu Re} \right]^{-2/3} N^{-2/3} t^{-2/3}, \tag{3.8}$$

where all the constants on the right-hand side of the equation are obtained directly from experiment. The values of K thus determined are shown in figure 5. The theory predicts that $K(N, Re)$ should be a constant for a cluster of a given shape, but there is some dependence of the experimentally determined K on both N and Re. More importantly, however, the curves for different Re do asymptote to a constant in the limit of large N, where the theoretical assumption of a continuum presentation becomes rigorously valid. The N dependence may be approximated by the simple form

$$K(N, Re) = \frac{c(Re)}{N} + K_0, \tag{3.9}$$

where c is a function only of Re and K_0 is a constant. The best fits to the values of K for the $Re = 93$ and $Re = 216$ runs are shown in figure 5, and yield $K_0 = 0.28\,(\pm 0.07)$ and $K_0 = 0.27\,(\pm 0.26)$, respectively (the ranges denote the 95 % confidence interval). Thus, the experimental value of the prefactor, in the limit of large N, appears to only be a weak function of Re and is about 0.25 in the range of Re investigated. The rather close correspondence between theory and experiment indicates that the data are consistent with both the $N^{2/3}$ and $t^{2/3}$ scaling predicted by theory. In addition, the asymptotic value of the experimental K, for large N is in the range suggested by theory, that is, $0.2 < K_0 < 0.42$. Given the rather arbitrary form of the fitting function and the error bars on K_0, it is difficult to make a definitive conclusion regarding whether the experimental clusters fall in the planar or spherical limit. Indeed, a value of $K = 0.25$ is between the two theoretical limits, consistent with the observations of non-planar clusters of aspect ratio less than unity (see § 2).

It is interesting to observe that the data in figure 5 for $Re = 93$ and $Re = 216$ agree quite well, and are both in accord with theory, although the flow around a single sedimenting particle is expected to lose its axisymmetry at about $Re = 100$. The agreement between experiments and theory for $Re = 216$ is therefore a little surprising, since, as mentioned earlier, the presence of a transverse lift must lead to a transverse drift, and therefore, a quadratic growth ($\langle r_t^2 \rangle \propto t^2$) in cluster dimensions. Unpublished data obtained at a later date (see A. Minnich, M. K. Rivera & R. E. Ecke, private communication, 2008) is indeed consistent with the onset of such an effect at slightly higher values of Re. However, for the range of Reynolds numbers examined here, effects related to the non-axisymmetry of the particle wakes appear to remain small over the duration of an experimental run (as is evident from figure 5, the experiments at the highest Re ($Re = 425$) were not carried out for large enough N in order for one to be certain about the value of K_0).

4. Conclusions

We have presented experimental evidence that clusters of 10–80 particles, having Reynolds numbers between 93 and 425, exhibit a mean-square horizontal size that grows with time as $t^{2/3}$ for large t, suggesting that the long-time growth of the cluster is a self-similar process. This observation is consistent with a theoretical analysis which attributes the spread to the source-flow hydrodynamic disturbances produced by the sedimenting particles at large distances. The change in the ratio $\langle r_t^2 \rangle / t^{2/3}$ with particle Reynolds number is consistent with the theoretical prediction that this ratio should be proportional to $Q^{2/3}$, where $Q = F_D/U$ is the source strength predicted by an Oseen flow analysis of the disturbance flow generated by a particle. The theoretical analysis indicates that clusters may grow as spheres or as planar arrays depending on the initial size of the cluster and the number of particles. Further, the theory predicts the same temporal scaling for the growth of spherical and planar clusters but a different prefactor K. Experiments yield a prefactor that lies in between the theoretical predictions for planar and spherical clusters, and thereby reinforce the fact that the predictions for spherical and planar clusters may serve as lower and upper bounds for the growth rate of an arbitrary cluster.

Most previous theoretical and experimental investigations attempting to elucidate the consequences of detailed hydrodynamic interactions among finite-Reynolds-number particles have addressed the situation of an unbounded homogeneous sedimenting suspension (see, for example, Koch 1993; Yin & Koch 2007). On the other hand, the analysis of finite-sized clusters of particles at finite Re offers insight

into the evolution of an inhomogeneous particulate system under the influence of hydrodynamic interactions. In fact, among earlier efforts, only the work of Bretherton (1964) pertains to a finite group of particles interacting at separations greater than the inertial screening length. Bretherton, however, considered expanding polygonal arrays with the interacting particles located at the vertices of the polygon. In our theoretical analysis (see Subramanian & Koch 2008), both the particle number density and velocity fields in the evolving cluster are unknowns, and must be solved for in order to obtain the rate of expansion. Since the particles' source-flow interactions lead to an increase in the radial extent of a cluster, this then provides a mechanism by which a localized release of particles into a quiescent fluid may lead to a sediment covering a larger portion of the bottom surface than would be supposed in the absence of hydrodynamic interactions. The analysis described here may thus be relevant to the dynamics of particulate gravity currents; the latter have applications to many geological (lava flows from volcanic eruptions), oceanographic (turbidity currents) and environmental (pollutant-laden industrial effluents) situations (see Bonnecze, Huppert & Lister 1993; Bonnecaze *et al.* 1995; Huppert 2006). The increased bulk density of the particulate current, due to the suspended particles, provides the driving buoyancy force for its spreading into a lighter ambient fluid. Further, such currents are usually characterized by high Reynolds numbers, and therefore evolve under a balance of inertial and buoyancy forces. For a turbidity current propagating in an aqueous environment, the Reynolds numbers of the suspended particles are no longer small, and microscale inertial forces also assume importance. Unlike homogeneous gravity currents, however, particle-driven gravity currents suffer a continuous loss of buoyancy through particle sedimentation. In all of the aforementioned applications, it is therefore of interest to determine the eventual run-out length of the current, and the silt deposit pattern resulting from such sedimentation. The models usually employed to study these systems neglect the detailed particle–particle hydrodynamic interactions, and the loss of buoyancy is modelled solely via a vertical efflux of particles sedimenting with a velocity corresponding to the Stokes sedimentation of an isolated particle. The analysis of repulsive finite Re interactions between sedimenting particles in this paper suggests their role as an additional mechanism in determining the buoyancy of a particle-laden gravity current.

This work was supported by NSF grant CBET-0730579.

REFERENCES

Batchelor, G. K. 1967 *Introduction to Fluid Dynamics*. Cambridge University Press. 351 pp.

Bonnecaze, R. T., Hallworth, M. A., Huppert, H. E. & Lister, J. R. 1995 Axisymmetric particle-driven gravity currents. *J. Fluid Mech.* **294**, 93.

Bonnecaze, R. T., Huppert, H. E. & Lister, J. R. 1993 Particle-driven gravity currents. *J. Fluid Mech.* **250**, 339.

Bretherton, F. P. 1964 Inertial effects on clusters of spheres falling in a viscous fluid. *J. Fluid Mech.* **20**, 401.

Clift, R., Grace, J. R. & Weber, M. E. 1978 *Bubbles, Drops and Particles*. Academic Press.

Feng, J., Hu, H. H. & Joseph, D. D. 1994 Direct simulation of initial-value problems for the motion of solid bodies in a Newtonian fluid. 1. Sedimentation. *J. Fluid Mech.* **261**, 95.

Fortes, A. F., Joseph, D. D. & Lundgren, T. S. 1987 Nonlinear mechanics of fluidization of beds of spherical particles. *J. Fluid Mech.* **177**, 467.

Ghidersa, B. & Dusek, J. 2000 Breaking of axisymmetry and onset of unsteadiness in the wake of a sphere. *J. Fluid Mech.* **423**, 33.

Huppert, H. E. 2006 Gravity currents: a personal perspective. *J. Fluid Mech.* **554**, 299.

Jenny, M., Dusek, J. & Bouchet, G. 2004 Instabilities and transition of a sphere falling or ascending freely in a Newtonian fluid. *J. Fluid Mech.* **508**, 201.

Koch, D. L. 1993 Hydrodynamic diffusion in dilute sedimenting suspensions at moderate Reynolds numbers. *Phys. Fluids* A **5**, 1141.

Magarvey, R. H. & Bishop, R. L. 1961 Transition ranges for 3-dimensional wakes. *Phys. Fluids* **39** (10), 1418.

Mittal, R. 1999 Planar symmetry in the unsteady wake of a sphere. *AIAA J.* **37**(3), 388.

Natarajan, R. & Acrivos, A. 1993 The instability of the steady flow past spheres and disks. *J. Fluid Mech.* **254**, 323.

Nitsche, J. M. & Batchelor, G. K. 1997 Break-up of a falling drop containing dispersed particles. *J. Fluid Mech.* **340**, 161.

Ormieres, D. & Provensal, M. 1999 Transition to turbulence in the wake of sphere. *Phys. Rev. Lett*. **83** (1), 80.

Subramanian, G. & Koch, D. L. 2008 Evolution of clusters of sedimenting low-Reynolds-number particles with Oseen interactions. *J. Fluid Mech.* **603**, 63.

Wu, J. S. & Faeth, G. M. 1993 Sphere wakes in still surroundings at intermediate Reynolds-numbers. *AIAA J.* **31** (8), 1448.

Yin, X. & Koch, D. L. 2007 Hindered settling velocity and microstructure in suspensions of spheres with moderate Reynolds number. *Phys. Fluids* **19**, 093302.